

Prediction of hot tearing during alloy solidification

J. Guo and J.Z. Zhu

ESI US R&D, 6851 Oak Hall Lane, Suite 119, Columbia, MD 21045, USA

Abstract

In order to predict the mechanical properties of an in-service part, it is very important to understand the relationships between the alloy chemistry, the processing, and the final properties. Such prediction is possible to a certain degree from given knowledge of the microstructure, phase fractions, and defects present in a metallic part. Hot tearing is one of the most serious defects for a casting. It is believed that this phenomenon occurs in the late stages of solidification. In this paper, a hot tearing indicator, which is based on the accumulated plastic strain in the last stage of solidification, was introduced to evaluate susceptibility to hot tearing during casting solidification processes. The last stage of solidification is studied. This includes the solidification ending temperature, thermal and mechanical properties, and alloy chemistry and cooling history are considered. The predictions are validated by comparison with experimental measurements.

Keywords: Late stages of solidification, hot tearing, back diffusion, thermodynamic modelling, Mg-Al alloys.

1. Introduction

Simulation technologies are applied extensively in casting industries to understand aspects of heat transfer and fluid transport phenomena and their relationships to the microstructure, the formation of defects [1], and occasionally the final mechanical properties. Hot tearing is a common defect encountered in castings. Eskin *et al.* [2] gave a very detailed review of hot tearing. It is believed that this phenomenon occurs in the late stages of solidification when the fraction solid is close to one. The alloy composition, casting geometry, cooling history, and mechanical properties of the casting are all related to the formation of hot tearing. The correlation between susceptibility to hot tearing and alloy composition is well established. The relationship between hot tearing and mechanical properties is easy to understand.

In order to predict the formation of hot tearing which occurs in the last stage of solidification, it is critical to have accurate thermophysical and mechanical properties, especially for the mushy zone, as input for complex solidification processes. The solidification path and thermophysical properties can be calculated with the help of thermodynamic calculations of phase stability at given temperatures and compositions. A comprehensive multi-component alloy solidification model, coupled with a Gibbs free energy minimization engine and thermodynamic databases, has been developed. A back-diffusion model is integrated so that the solidification conditions, such as cooling rate, can be taken into account.

Much research has been done on the formation of hot tearing. Proposed mechanisms of hot tearing can be found in the literature (see, e.g., [2] and the references therein). Most of the existing theories of hot tearing are based on

the development of strain, strain rate, or stress in the semi-solid state of the casting. For strain-based theory, it is believed that hot tearing will occur when the accumulated strain exceeds its ductility [3–5]. Strain rate-based theories suggest that hot tearing may form when the strain rate, or strain rate related pressure, reaches its critical limit during solidification [6,7]. Stress-based criteria, on the other hand, assume that hot tearing will start if the induced stress in the semi-solid exceeds some critical value [8,9]. These theories can be considered as somewhat related due to the fact that strain, strain rate and stress are themselves related. Such a relationship motivates us to develop a hot tearing indicator, which uses the accumulated plastic strain as an indication of susceptibility to hot tearing by considering the evolution of strain, strain rate and stress in the last stage of solidification, for the numerical simulation of solidification. We believe that the hot tearing indicator presented in our discussion can also be generalized to much wider applications.

To compute an effective hot tearing indicator, it is important to have accurate inputs, so that the casting chemistry, casting geometry, and the cooling history can be properly considered. In this paper, back diffusion thermodynamic calculation for some binary Mg-Al alloys are given first so that the solidification path can be predicted accurately, followed by the thermophysical and mechanical properties calculation for those alloys. A hot tearing indicator is introduced next. Some experimental validations are performed in the end.

2. Thermodynamic calculation

Solidification proceeds at various rates. The solidification path determines the solidification behavior for an alloy. For

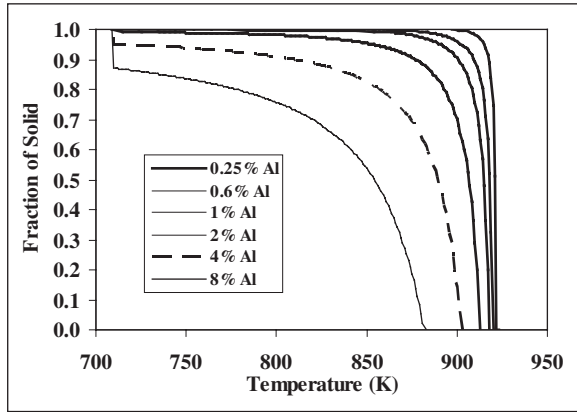


Figure 1: Solidification path for different binary Mg-Al alloys based on 100 K/s cooling rate and a back diffusion thermodynamic calculation.

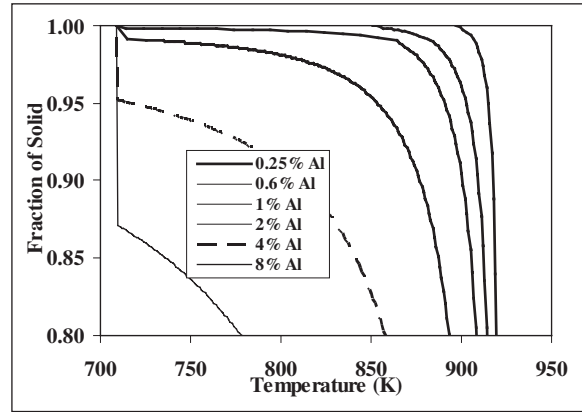


Figure 2: Last stage of solidification for different binary Mg-Al alloys based on 100 K/s cooling rate and a back diffusion thermodynamic calculation.

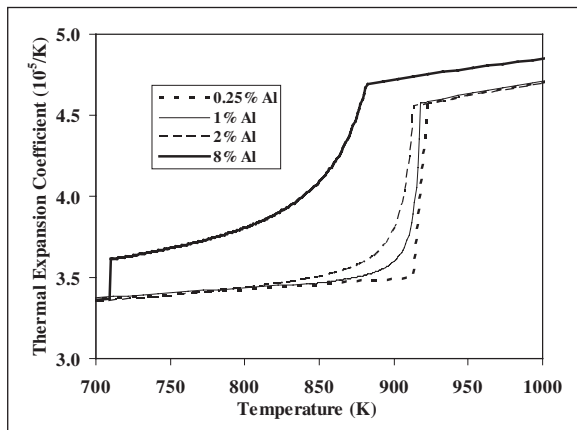


Figure 3: Thermal expansion coefficient variation with temperature for different alloys.

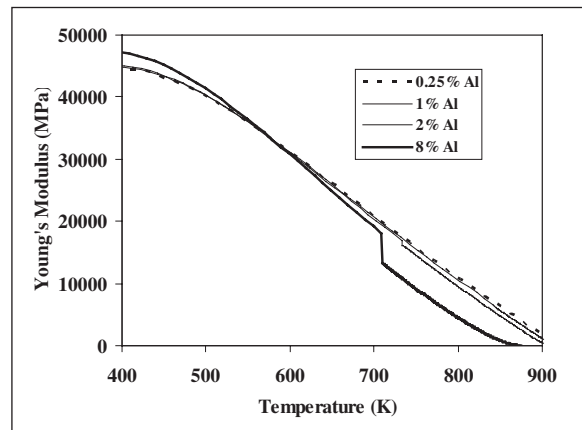


Figure 4: Young's modulus variation with temperature for different alloys.

complex multi-component alloys, the solidification path is very complicated. Hence the equilibrium of each phase at different temperature needs to be calculated. The thermodynamics as well as the kinetics calculation is the basis for the prediction of solidification. The diffusive transport in the solid phase needs to be solved for each element. This requires knowledge of the diffusion coefficient, the length scale, and the cooling conditions. Recently, thermodynamic modeling has become increasingly used to predict the equilibrium and phase relationships in multi-component alloys [1,10,11]. Back diffusion is included for all elements in the solidification calculation. Cooling rate is taken into account in this model. Further detailed information about the back diffusion thermodynamic calculation can be found in [12]. Here solidification of several binary Mg-Al alloys is investigated during die casting process. For a die casting, the cooling rate is around 100 K/s. Figure 1 shows the solidification paths of Mg-Al alloys with 0.25, 0.6, 1.0, 2.0, 4.0, and 8.0 wt% aluminum, at 100 K/s cooling rate. The last stage of solidification of these alloys is shown in Figure 2. It can be seen that the start and end solidification temperatures are quite different for different alloy compositions. Based on the Scheil model, the ending solidification temperature will be the eutectic temperature for these binary Mg-Al alloys. Because of back diffusion, not all of the ending solidification

temperatures for these alloys, such as Mg-0.25%Al and Mg-0.6%Al, are at the eutectic temperature. The temperature differences between fraction solid at 0.9 and end of solidification are quite different between these alloys too. Since hot tearing occurs in the last stage of solidification, obviously this difference can affect the hot tearing calculation greatly.

3. Thermophysical and mechanical properties calculation

To obtain the thermophysical properties experimentally at low temperature can be time consuming and expensive. It becomes even more difficult at high temperature especially when close to or above the solidus temperature. With the help of thermodynamic calculation, the thermophysical properties can be predicted [1]. An extensive database for the calculation of thermophysical properties has been developed which utilizes the phase fraction information predicted with the minimization routines developed by Lukas *et al.* [10] and extended by Kattner *et al.* [11]. These properties include density, specific heat, enthalpy, latent heat, electrical conductivity and resistivity, thermal conductivity, liquid viscosity, Young's modulus, and Poisson's ratio. The thermodynamic calculation is based on the thermodynamic

database from CompuTherm LLC (Madison, WI 53719 USA). A simple pair-wise mixture model which is similar to that used to model thermodynamic excess functions in multi-component alloys is used to calculate the properties [1].

$$P = \sum_i x_i P_i + \sum_i \sum_{j>i} x_i x_j \sum_v \Omega_v (x_i - x_j)^v \quad (1)$$

where P is the phase property, P_i is the property of the pure element in the phase, Ω_v is a binary interaction parameter, and x_i and x_j are the mole fractions of elements i and j in that phase.

Because of the different amounts of Al and the different solidification paths, the density curves are very different for these alloys. Based on the density calculation, the thermal expansion coefficients are calculated and shown in Figure 3. Figure 4 shows the calculated Young's modulus values. The calculated data is used for the thermal, fluid flow, and stress analyses.

4. Hot tearing indicator

The constitutive model used to describe the material behavior in the semi-solid state is the Gurson model [13–15], which was originally developed for studying the progressive micro-rupture through nucleation and growth of micro-voids in a ductile and porous solid.

When the material is considered as elastic-plastic, the yield condition in the Gurson model is of the form

$$\phi(\sigma, \mathbf{x}, T, \bar{\epsilon}^P, G_u) = F(\sigma) - G_u(\sigma, \bar{\epsilon}^P, f_v) \kappa(\bar{\epsilon}^P, T) = 0 \quad (2)$$

where $F(\sigma) = (3(\mathbf{s} - \mathbf{x}) : (\mathbf{s} - \mathbf{x})/2)^{1/2}$ is the Mises stress in terms of the deviatoric stress $\mathbf{s} = \sigma - (tr\sigma)\mathbf{I}/3$, κ represents the plastic flow stress due to isotropic hardening, and \mathbf{x} denotes back stress due to kinematic hardening. The accumulated effective plastic strain is written as

$$\bar{\epsilon}^P = \int_0^t \sqrt{(2/3) \dot{\epsilon}^P : \dot{\epsilon}^P} d\tau \quad (3)$$

with
$$\dot{\epsilon}^P = \dot{\gamma} \frac{\partial \phi}{\partial \sigma} \quad (4)$$

and $\dot{\gamma}$ being the plastic flow parameter. The Gurson coefficient G_u is defined as

$$G_u = -2f^* q_1 \cosh\left(\frac{tr(\sigma)}{2\kappa}\right) + \{1 + (q_1 f^*)^2\} \quad (5)$$

in which, q_1 is a material constant and

$$f^* = f_v \quad \text{for } f_v \leq f_c$$

$$f^* = f_c + \frac{f_u - f_c}{f_F - f_c} (f_v - f_c) \quad \text{for } f_v > f_c \quad (6)$$

Here, $f_u = 1/q_1 f_c$ is the critical void volume fraction and f_F is the failure void volume fraction. Following Tvergaard and Needleman [14], their values are chosen as $q_1 = 1.5$, $f_c = 0.15$, and $f_F = 0.25$. The Gurson coefficient characterizes the rapid loss of material strength due to the growth of void volume fraction f_v . When $f_v = f_F$ then $f^* = f_u = 1/q_1$, we have $G_u = 0$, for zero stress, i.e., the stress carrying capacity of the material vanishes.

The evolution of the void volume fraction is described by the nucleation of new voids and the growth of existing voids, i.e.

$$\dot{f}_v = \dot{f}_{nucleation} + \dot{f}_{growth} \quad (7)$$

with the rate of void growth defined as

$$\dot{f}_{growth} = (1 - f^*) tr(\dot{\epsilon}^P) = \dot{\gamma} (1 - f^*) \left(\frac{3f^* q_1}{\kappa}\right) \sinh\left(\frac{tr(\sigma)}{2\kappa}\right) \quad (8)$$

In our study, void nucleation is assumed to be strain controlled and is written as

$$\dot{f}_{nucleation} = \dot{\epsilon}_{ht} \quad (9)$$

where
$$e_{ht} = \int_{t_c}^t \sqrt{(2/3) \dot{\epsilon}^P : \dot{\epsilon}^P} d\tau \quad t_c \leq t \leq t_s \quad (10)$$

is defined as our *hot tearing indicator* (HTI). t_c represents time at coherency temperature and t_s denotes time at solidus temperature. It is observed that the hot tearing indicator is in fact the accumulated plastic strain in the semi-solid region and it corresponds to the void nucleation. Therefore, it should provide a good indication of the susceptibility to hot tearing during solidification. The value of the hot tearing indicator is determined by finite element analysis [16]. For materials described by viscoplastic or creep model, the yield condition does not exist. The function ϕ defined in Equation 2 can be used as a potential for the inelastic flow, so that the inelastic part of the strain rate is still given in the form of Equation 4.

5. Experimental validation

Cao *et al.* [17] performed an experiment to study the hot tearing formation during solidification of binary Mg-Al alloys in a steel mold. The steel mold is shown in Figure 5. It casts four 9.5 mm diameter rods of lengths 51, 89, 127, and 165 mm. There is a 19 mm diameter ball at the end of each rod to restrain the rod from free contraction during solidification.

A hot cracking susceptibility (HCS) was introduced which is a function of maximum crack width, crack length factor, and the crack location. It was found that it is easier to have cracks at the sprue end than at the ball end. It is less likely to crack in the middle of the rod. Also, the longer the rod the easier it is to have a crack. Figure 6 shows the simulated results of the hot tearing indicator for a Mg-2%Al alloy casting. The computed hot tearing indicator agrees very well with the experiments.

Figure 7 shows the experimental results of hot tearing at the sprue end of the rods for three different alloys. The calculated hot tearing indicators are shown in Figure 8 accordingly. It can be seen that hot tearing is less severe as the Al content increases from 2% to 4% and then to 8% at the same location for the same casting with the same casting conditions. Again, the simulated hot tearing indicators agree well with the observations. Figure 9 shows the hot cracking susceptibility (HCS) defined by Cao *et al.* [17] from their experiments. This susceptibility rises sharply from pure Mg, reaches its maximum at Mg-1%Al and decreases gradually with further increase in the Al content.

The hot tearing indicator is calculated at the end of sprue for the longest rod for different alloy compositions. For comparison, the hot tearing indicators as well as a crack susceptibility coefficient (CSC), which is defined as the temperature difference between fraction solid at 0.9

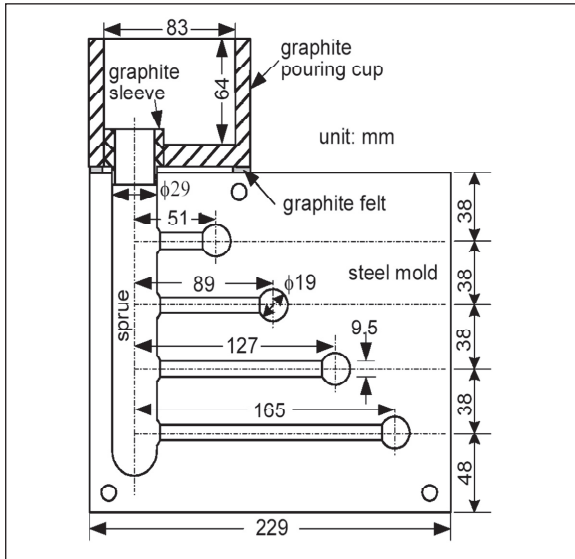


Figure 5: Steel mold for constrained rod casting [17].

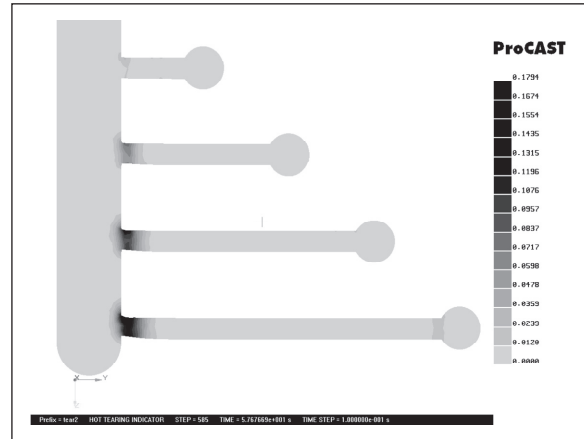


Figure 6: Hot tearing indicator for a Mg-2%Al alloy casting.

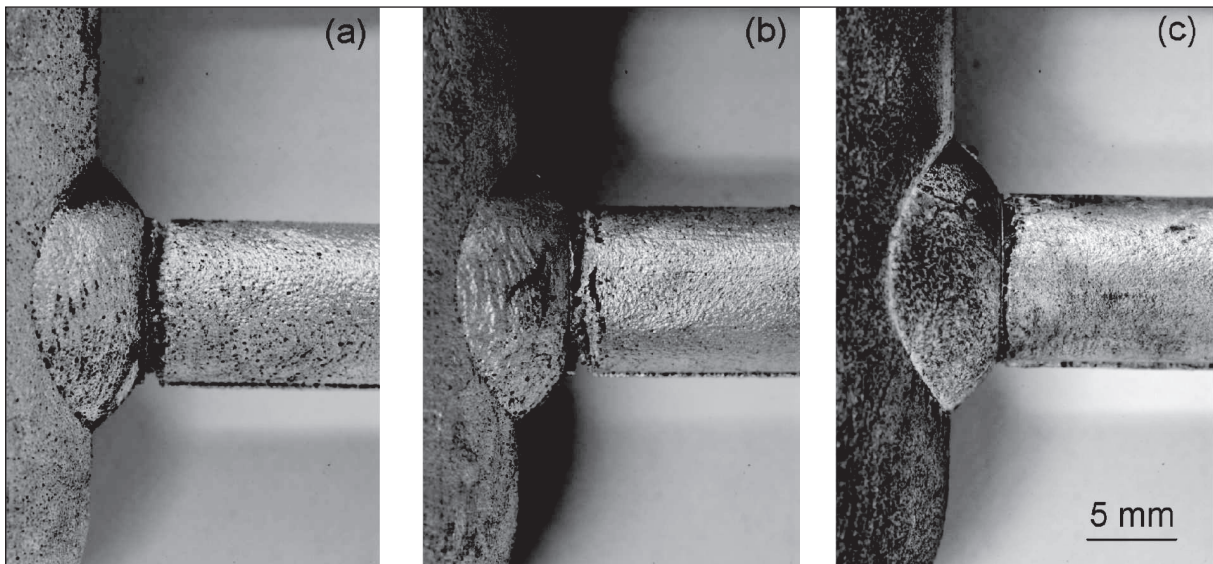


Figure 7: Close-up views of hot tears (cracks) in the bottom of rods near the sprue: (a) Mg-2%Al; (b) Mg-4%Al; (c) Mg-8%Al.

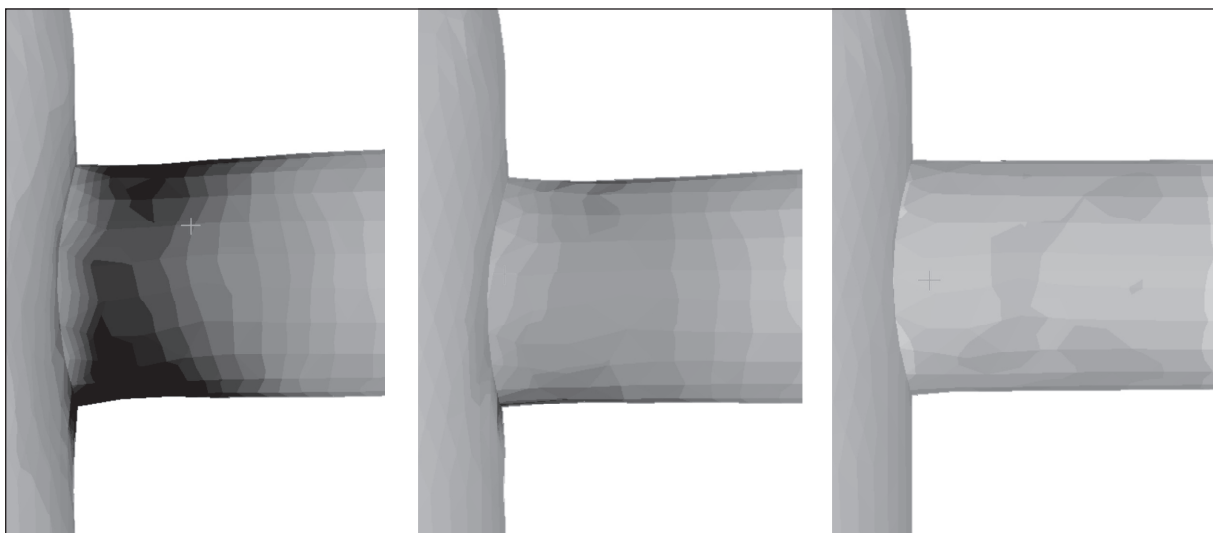


Figure 8: Hot tearing indicator in the bottom of rods near the sprue: (a) 2% Al; (b) 4% Al; (c) 8% Al.

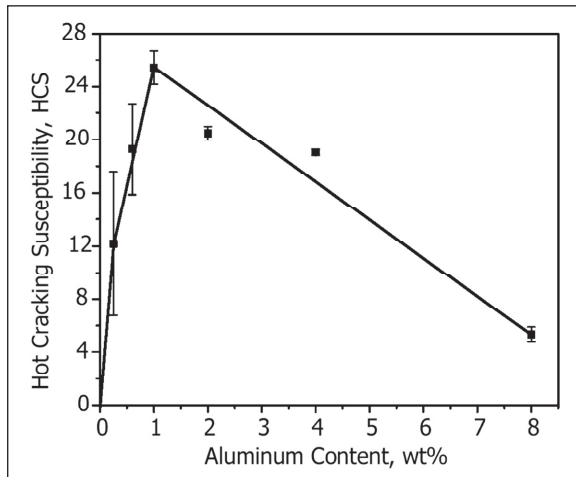


Figure 9: Hot cracking susceptibility vs. Al content for Mg-Al alloys [17].

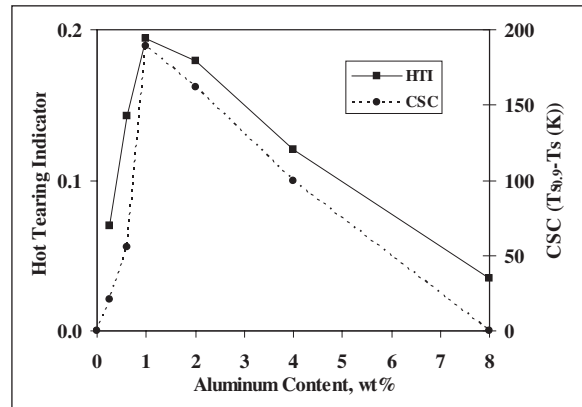


Figure 10: Comparison between the hot tearing indicator and crack susceptibility coefficient, both vs. Al content for Mg-Al alloys.

and at the end solidification, are shown in Figure 10. Just as in the experiment, the susceptibility to hot tearing rises sharply from pure Mg, reaches its maximum at Mg-1%Al and decreases gradually with further increase in the Al content. It tells us that the current hot tearing indicator can predict the trend of hot tearing formation very well. The alloy chemistry, casting geometry, and cooling conditions all contribute to the formation of hot tearing and they are included in this model directly or indirectly.

6. Conclusion

A comprehensive multi-component alloy solidification model, which is coupled with thermal-fluid-stress macro-models, has been developed and implemented in a commercial software code, ProCAST. The model can accurately predict formation of hot tearing during casting solidification. The alloy chemistry, casting geometry, and cooling conditions are all included in this model directly or indirectly. The predicted results agree well with the experiments. This model can be applied to multi-component casting alloys other than binary Mg-Al alloys as well.

References

1. J. Guo, and M.T. Samonds, in: *Modeling of Casting, Welding and Advanced Solidification Processes-X*, Edited by D.M. Stefanescu, et al., 2003, pp. 303–310.
2. D.G. Eskin, Suyitno, and L. Katgerman, *Progr. Mater. Sci.*, **49** (2004) 629–711.
3. B. Magnin, L. Maenner, L. Katgermann, and S. Engler, *Mater. Sci. Forum*, 1996, **1209**;217–22.
4. L. Zhao, B. Wang, V. Sahajwalla, and R.D. Pehlke, *Internat. J. Cast Metals Res.*, 2000, **13**(3);167.
5. W.S. Pellini, *Foundry*, 1952, **80**;124.
6. M. Rappaz, J.M. Drezet, and M. Gremaud, *Metall. Mater. Trans. A*, 1999, **30A**;449.
7. N.N. Prokhorov, *Russian Castings Production*, 1962, **2**;172.
8. C.H. Dickhaus, L. Ohm, and S. Engler, *AFS Trans.*, 1994, **101**;677.
9. J. Langlais and J.E. Gruzleski, *Mater. Sci. Forum*, 2000, **167**;331–7.
10. H.L. Lukas, J. Weiss, and E.Th. Henig, *CALPHAD*, **6**, No. 3, pp. 229–251 (1982).
11. U.R. Kattner, *JOM*, Dec. 1997, pp. 14–19.

12. J. Guo and M.T. Samonds, *J. Phase Equilibria and Diffusion*, in press, 2007.
13. A.L. Gurson, *J. Engng. Mater. Tech.*, 1977, **99**;2.
14. V. Tvergaard and A. Needleman, *Acta Metall.*, 1984, **32**;157.
15. A. Needleman and V. Tvergaard, *J. Mech. Phys. Solids*, 1987, **35**;151.
16. O.C. Zienkiewicz and R.L. Taylor, *The Finite Element Method: For Solid and Structural Mechanics*, 2005, Elsevier.
17. G. Cao, S. Kou, and Y.A. Chang, in: *Magnesium Technology 2006*, Edited by A.A. Luo et al., TMS, 2006, pp. 57–62. ■